AD-A081 592 IOWA STATE UNIV AMES ENGINEERING RESEARCH INST F/G 20/4
PREDICTION OF SEPARATING TURBULENT BOUNDARY LAYERS. INCLUDING RE--ETC(U)
FEB 80 R H PLETCHER, O K KWON, R CHILUKURI DAAG29-76-G-0155
UNCLASSIFIED ISU-ERI-AMES-80112 ARO -13376.4-E NL

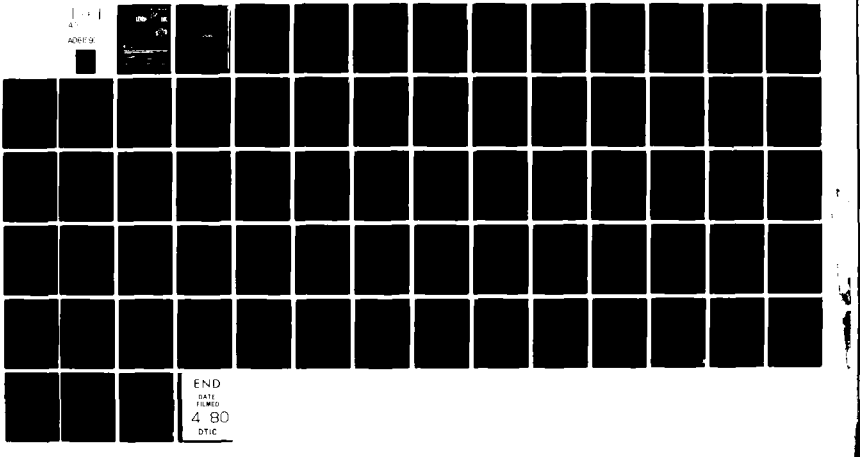

END
DATE FILMED
4 80
DTIC

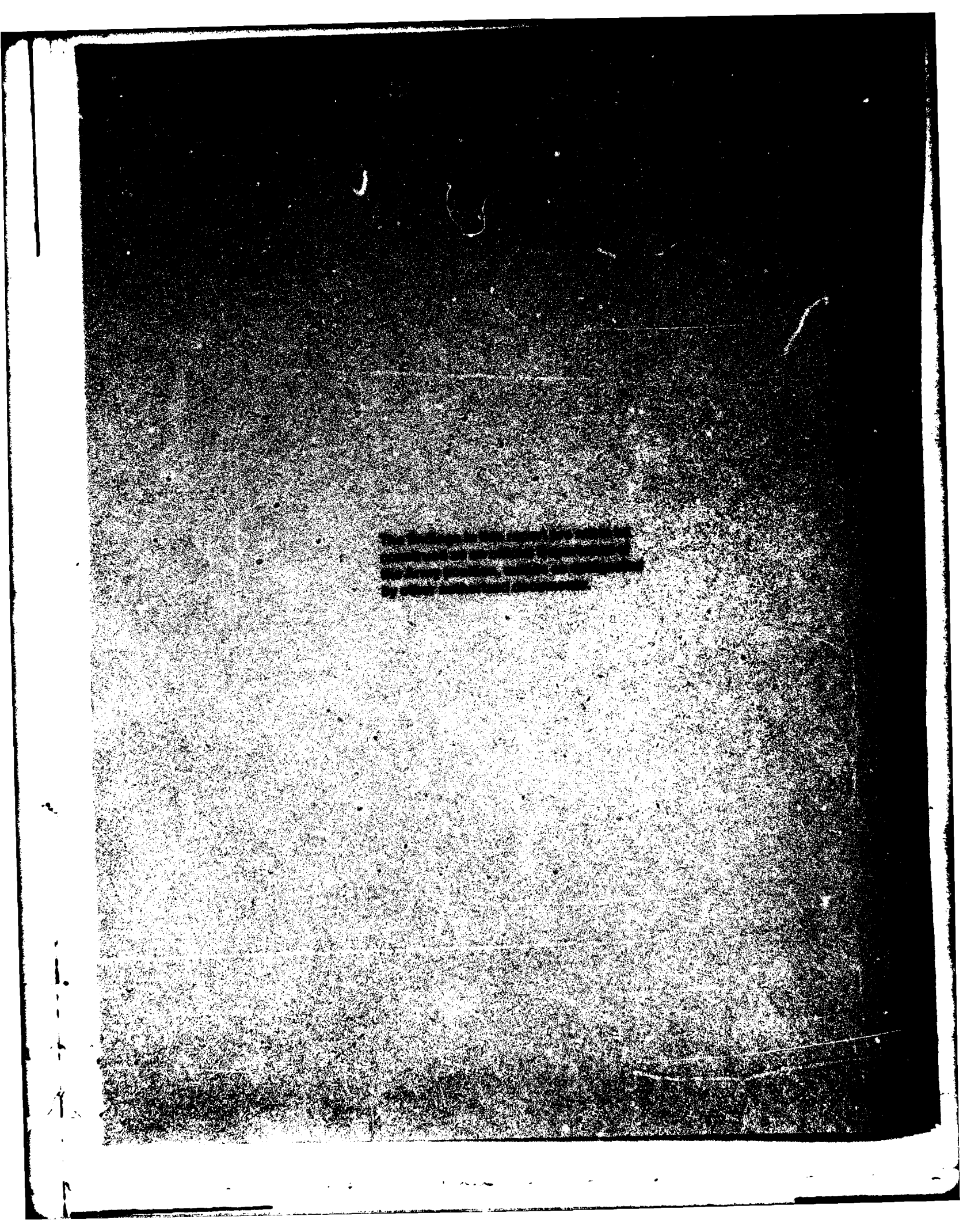

ENGINEERING RESEARCH

ENGINEERING RESEARCH
ENGINEERING RESEARCH
ENGINEERING RESEARCH
ENGINEERING RESEARCH

Final Technical Report

PREDICTION OF SEPARATING TURBULENT BOUNDARY LAYERS INCLUDING REGIONS OF REVERSED FLOW

R. H. Pletcher
O. K. Kwon
R. Chilukuri
February 1980

Prepared under
Grant DAAG29-76-G-0155
for the U.S. Army Research Office

HTL-22
ISU-ERI-Ames-80112
Project 1219

HEAT TRANSFER LABORATORY
DEPARTMENT OF MECHANICAL ENGINEERING
ENGINEERING RESEARCH INSTITUTE
IOWA STATE UNIVERSITY AMES, IOWA 50011

CLASSIFICATION OF THIS PAGE (When Data Entered)

REPORT DOCUMENTATION PAGE

READ INSTRUCTIONS BEFORE COMPLETING FORM

1. REPORT NUMBER: ISU-ERI-Ames-80112 (18) ARO
2. GOVT ACCESSION NO.
3. RECIPIENT'S CATALOG NUMBER: (19) 13376.4-E

4. TITLE (and Subtitle): (6) PREDICTION OF SEPARATING TURBULENT BOUNDARY LAYERS INCLUDING REGIONS OF REVERSED FLOW.

5. TYPE OF REPORT & PERIOD COVERED: (9) Final Technical Report.

6. PERFORMING ORG. REPORT NUMBER: HTL-22

7. AUTHOR(s): (10) R. H. Pletcher, O. K. Kwon, R. Chilukuri

8. CONTRACT OR GRANT NUMBER(s): (15) DAAG 29-76-G-0155

9. PERFORMING ORGANIZATION NAME AND ADDRESS: Heat Transfer Laboratory and Engineering Research Institute, Iowa State University, Ames, Iowa 50011

10. PROGRAM ELEMENT, PROJECT, TASK AREA & WORK UNIT NUMBERS

11. CONTROLLING OFFICE NAME AND ADDRESS: U. S. Army Research Office, Post Office Box 12211, Research Triangle Park, NC 27709

12. REPORT DATE: (11) Feb[illegible]80

13. NUMBER OF PAGES: 63

14. MONITORING AGENCY NAME & ADDRESS (if different from Controlling Office): (12) 72

15. SECURITY CLASS. (of this report): Unclassified

15a. DECLASSIFICATION/DOWNGRADING SCHEDULE: NA

16. DISTRIBUTION STATEMENT (of this Report)

Approved for public release; distribution unlimited.

17. DISTRIBUTION STATEMENT (of the abstract entered in Block 20, if different from Report)

NA

(14) ISU-ERI-AMES-80112, HTL-22

18. SUPPLEMENTARY NOTES

The findings in this report are not to be construed as an official Department of the Army position, unless so designated by other authorized documents.

19. KEY WORDS (Continue on reverse side if necessary and identify by block number)

Turbulent flow, separated flow, turbulence modeling, viscous-inviscid interactions, finite-difference methods.

20. ABSTRACT (Continue on reverse side if necessary and identify by block number)

The results of a research program to develop and evaluate improved prediction methods for turbulent separating flows are summarized. The predictions of several turbulence models have been compared with experimental data for flows containing regions of recirculation using an inverse finite-difference method to solve the boundary layer equations. A new turbulence model which employs a one-dimensional transport equation for the outer-layer length scale was seen to provide the best agreement with the experimental data beyond

DD FORM 1 JAN 73 1473 EDITION OF 1 NOV 65 IS OBSOLETE

404410

Unclassified

SECURITY CLASSIFICATION OF THIS PAGE (When Data Entered)

separation. A viscous-inviscid interaction calculation procedure was developed to predict airfoil flows containing leading edge or midchord separation bubbles. The procedure utilized the inverse finite-difference method to predict the viscous flow and a small disturbance Cauchy integral formulation for the inviscid flow. Three models for laminar-turbulent transition were evaluated. Generally good agreement between predictions of the best model and measurements was observed in the several comparisons made. Some early results from a finite-difference scheme to solve the partially parabolized Navier-Stokes equations in primitive variables were also reported. The method was developed to predict viscous flows in which normal pressure gradients cannot be neglected. Good agreement between the predictions and numerical solutions to the full Navier-Stokes equations for developing laminar channel flow at Reynolds numbers as low as 10 and a nearly separating laminar external flow at a Reynolds number of approximately 10^4 was noted.

TABLE OF CONTENTS

LIST OF FIGURES

LIST OF TABLES

NOMENCLATURE

A	function of Mach number (see Eq. 3.8)
b_0, b_1	constants
C	constant
c	airfoil chord
C_p	pressure coefficient, $1 - (u_e/u_\infty)^2$
M	Mach number
p	pressure
q	intensity of line source or sink
R	reattachment point
Re_x	Reynolds number based on x
Re_θ	Reynolds number based on momentum thickness
S	separation point
s	distance along upper surface of airfoil measured from stagnation point
s'	distance along surface measured from leading edge
Tu	freestream turbulence level, $100[(\overline{u'^2} + \overline{v'^2} + \overline{w'^2})/3]^{1/2}/u_\infty$
u	x component of velocity
v	y component of velocity
x	coordinate along the surface
x^*	dimensionless distance, $b_1 x/b_0$
x'	variable of integration in Eq. 3.3
x_1	interaction starting point
x_2	interaction end point
Δx	length of transition region
y	coordinate normal to surface

y_e	distance to outer boundary
γ	intermittency function
δ	boundary layer thickness
δ^*	displacement thickness, $\int_0^\infty (1 - u/u_e)dy$
λ	extent of transition region
μ	viscosity
ν	kinematic viscosity
ζ	normalized streamwise coordinate in transition zone, $(x - x_{tr})/\lambda$
ρ	density
τ	shearing stress

Subscripts

BL	denotes boundary layer
c	indicates value of correction
e	evaluated at outer flow boundary
ft	evaluated for fully turbulent flow
INV	denotes inviscid flow
L	evaluated at downstream flow boundary
n	denotes iteration level
o	denotes reference quantity
s	denotes evaluation at separation point
t	denotes turbulent flow quantity or transition end point
tr	denotes transition initiation point
∞	denotes evaluation at freestream conditions far upstream of airfoil

Superscripts

$\bar{(\ )}$	bars on dependent variables denote time mean quantities
$(\ )'$	prime on dependent variables denote fluctuations

1. INTRODUCTION

The prediction and control of turbulent flow separation and reattachment continue to be important in many engineering applications. Subsonic flow separation occurs or can occur in many important engineering devices such as airfoils, helicopter blades, near the tail of axisymmetric bodies, ship hulls, and in diffusers, compressors, and engine inlets. In many applications it is desirable to avoid separation entirely. In others, some separated regions must be tolerated over some range of the operating conditions; and it is highly desirable to be able to predict performance even with regions of recirculation present. Although progress is being made in the understanding and prediction of these flows, the accurate and economical calculation of turbulent flows containing regions of recirculation still remains one of the major challenges in the field of computational fluid dynamics.

Most recent investigators dealing with separated flows have been optimistic that the boundary layer equations may provide a suitable mathematical description for at least thin separated regions at moderate or high Reynolds numbers. However, care must be taken in the solution of boundary layer equations for separated flows. Conventional "direct" solution procedures for attached flows specify the pressure gradient as part of the outer boundary condition. This solution procedure becomes singular at separation. Goldstein first brought attention to this singularity in 1948 [1]. The manner in which this singularity appears in finite-difference solutions was illustrated by Pletcher and Dancey [2]. In recent calculations with boundary layer equations, the

singularity has been avoided for subsonic flows by employing an "inverse" procedure whereby the displacement thickness or wall shear stress is specified in lieu of the pressure gradient [3,4,5], or by providing an interaction equation (usually coupled with a solution for the inviscid outer flow) by which the pressure gradient can adjust simultaneously with the solution [2,6,7].

Apart from the separation point singularity, the flow reversal prevents the once-through solution of the difference equations without special attention being given to the evaluation of the convective terms in the momentum equation. The approximate treatment of the streamwise derivative suggested by Reyhner and Flügge-Lotz [8] has enabled several investigators [2,4,5] to compute through regions of recirculation in a single pass.

Several investigators [9,10,11,12] have employed a more exact evaluation of the troublesome convective terms for the recirculating region in laminar flows by making multiple computational sweeps of the flow field in an iterative fashion. However, to date, the evidence tends to suggest that the Reyhner-Flügge-Lotz (FLARE) approximation is a fairly good one when the maximum reversed flow velocities are less than about 10% of the velocity in the outer stream [10], a range that includes many, if not most, separated flows of interest in aerodynamic applications. The use of this approximation can result in significant computational savings.

The solution of boundary layer equations alone provides only part of the answer to the problem posed by separation in applications because

information from or at least compatible with the outer inviscid flow is needed to establish the outer boundary conditions for this boundary layer calculation. In the neighborhood of separation, the inviscid flow solution over the displacement surface of the viscous flow significantly differs from the inviscid flow over the solid body alone. Neither the correct inviscid solution nor the correct viscous flow solution can be obtained independently. The two problems must be solved simultaneously or iteratively until the solutions "match" through a common streamwise pressure gradient at the solid surface. Thus, a practical calculation scheme based on boundary layer equations must include provisions for the viscous-inviscid interaction.

There have been relatively few reports of viscous-inviscid interaction schemes applied to subsonic separated turbulent flow. Interaction methods based on an integral procedure for the viscous flow have been applied to fully-stalled turbulent flow in diffusers [13] and to the flow over a rearward-facing step in an internal flow [14]. Crimi and Reeves [15] also used an integral analysis in developing a prediction scheme for leading edge separation bubbles. Gerhart and Chima [16] reported that an attempt to apply an integral boundary layer scheme in an interaction procedure for treating subsonic turbulent separation had, to date, been unsuccessful. Differential solutions to the boundary layer equations were used in the interaction schemes applied to subsonic turbulent flow by Briley and McDonald [17], Carter [18], and Kwon and Pletcher [19]. The Briley and McDonald study utilized a time-dependent analysis, whereas both Carter and Kwon and Pletcher employed inverse

boundary layer procedures. Carter [18] computed the separated flow on an axisymmetric body-sting juncture, whereas the other two studies [17,19] treated transitional midchord separation bubbles. Only [17] and [19] included comparisons with experimental data.

Considerable uncertainty still exists in predicting separated turbulent flows. For many years, boundary layer equations were thought to be an unsuitable vehicle for analysis of separated flows either because of questions concerning the order of magnitude in terms neglected or because of the apparent impossibility of obtaining solutions because of a number of difficulties, including the separation point singularity. This latter impediment has now been eased, but a question remains about the accuracy limits of the boundary layer approximation for separated flows. The question is clouded somewhat by equal if not greater uncertainty about appropriate turbulence models for these flows.

This report describes the results of a research program to develop and evaluate improved methods of predicting turbulent boundary layer flows in the neighborhood of separation, including the region of recirculation downstream of separation. Three distinct phases of this study can be identified:

1. Development and application of an inverse boundary layer finite-difference scheme to evaluate suitable turbulence models for external flows with regions of flow reversal.
2. Development of a viscous-inviscid interaction prediction method for separating flows.

3. Development of a calculation scheme which includes pressure variations in the normal direction.

The results of these studies will be summarized in the following sections.

2. PREDICTION OF TURBULENT SEPARATING FLOW

An inverse finite-difference boundary layer prediction scheme was developed to permit the calculation of turbulent flows beyond separation. Conventional finite-difference schemes specify the pressure gradient (or alternatively, u_e) as an outer boundary condition. This conventional procedure is often referred to as a "direct" method. The direct procedure gives a solution which is known to be singular at the separation point as demonstrated by Pletcher and Dancey [2] and others. In an "inverse" procedure, some other condition on the solution, such as the displacement thickness, wall shear stress or the normal component of velocity at the outer edge, is specified instead of the pressure gradient. As long as specification of the pressure gradient is avoided, the solution procedure appears to be non-singular at the separation point. The essential features of the inverse method for separated flows employed in the present research and reported in detail in [3] will be summarized below.

2.1. Analysis

The flow is assumed to be two-dimensional, steady, and incompressible. Any separated regions are assumed to be sufficiently thin so that the boundary layer form of the momentum and continuity equations provides a good but approximate model for the forward-going flow. In any region of reversed flow, the streamwise convective derivative is also assumed to be negligibly small. Neglecting turbulent normal stresses, the governing conservation equations are:

Continuity

$$\frac{\partial u}{\partial x} + \frac{\partial v}{\partial y} = 0 \tag{2.1}$$

Momentum

$$C\left|u\right|\frac{\partial u}{\partial x} + v\,\frac{\partial u}{\partial y} = -\frac{1}{\rho}\,\frac{dp}{dx} + \frac{1}{\rho}\,\frac{\partial \tau}{\partial y} \tag{2.2}$$

where $C = 1.0$ when $u > 0$, and C = a small (≤ 0.2) positive constant when $u \leq 0$ and

$$\tau = \mu\,\frac{\partial u}{\partial y} - \rho\overline{v'u'} \tag{2.3}$$

The inner boundary conditions are

$$u(x,0) = v(x,0) = 0 \tag{2.4}$$

For attached flows some distance from the separation point, the standard direct finite-difference method was employed for which the outer boundary condition was

$$\lim_{y\to\infty} u(x,y) = u_e(x) \tag{2.5}$$

For the inverse method, the second boundary condition satisfied by the streamwise component of velocity was

$$\int_0^\infty \left(1 - \frac{u}{u_e}\right) dy = \delta^*(x) \tag{2.6}$$

where $\delta^*(x)$ is a prescribed function.

Equation (2.2) deviates from the conventional momentum equation in the treatment (FLARE approximation, [8]) of the streamwise derivative term, $C|u|\frac{\partial u}{\partial x}$. The form used permits marching the solution through regions of reversed flow by avoiding a negative coefficient for the streamwise derivative term. As indicated in the Introduction, evidence accumulated by several investigations indicates that this approximation is a valid one for flows in which the reversed flow velocities are small. This point is discussed further in [3].

2.2. Turbulence Modeling

The objective of this phase of the study was to identify the simplest turbulence model that would provide reasonable predictions of mean flow quantities in regions where separation had occurred. The strategy was first to evaluate the predictions of the simpler algebraic turbulence models and determine, where possible, the primary cause for any poor performance detected in terms of model parameters, and then to "correct" the problem by moving to a more complex model capable of providing a satisfactory distribution for the model parameter most obviously at fault. Five models were evaluated in [3] by comparing predictions with the measurements of Simpson et al. [20] and Chu and Young [21], which included data beyond the separation point. Figure 1 shows a representative velocity profile comparison well into the separated region of the measurements reported by Simpson et al. [20]. The models referred to in the figure can be briefly described as follows:

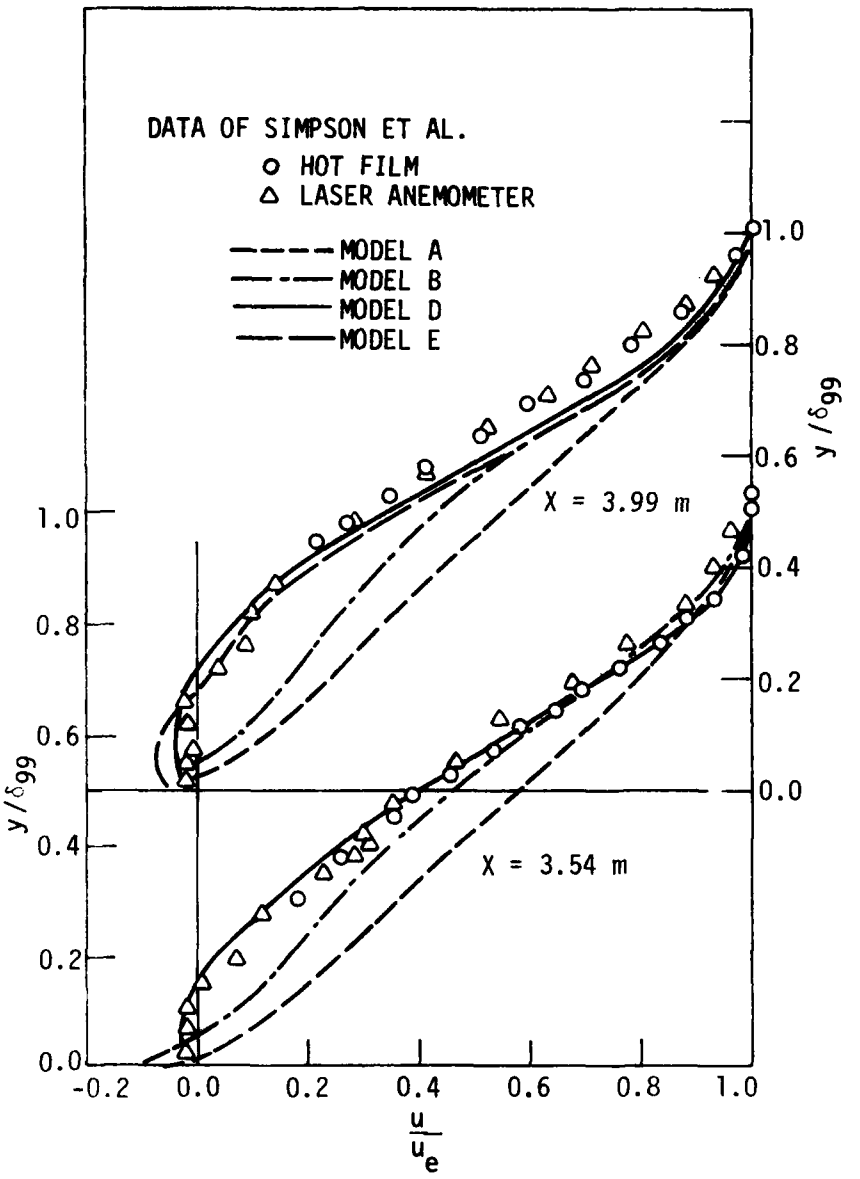

Fig. 1. Comparison of predicted and experimental [20] velocity profiles for a turbulent boundary layer with reversed flow.

- Model A. Simple mixing-length model used as baseline (Model 2 of [22]).
- Model B. Cebeci-Smith model (Model 1 of [22]).
- Model C. A turbulence kinetic energy model (similar to the Prandtl energy model).
- Model D. Model A supplemented with the newly developed length scale transport equation.
- Model E. Model D augmented by the use of a solution to the turbulent kinetic energy equation.

Models D and E originated during the present study. A comparison of the predictions of Model A and D illustrates the level of improvement which can be attributed to the use of the new length scale transport equation. Details of all of these models, as well as a description of the finite-difference solution method, can be found in [3].

2.3. Summary of Results

Several comparisons of predictions with the experimental measurements of [20] and [21] are given in [3], both for flows approaching separation and for those containing recirculating regions.

Relatively standard algebraic turbulence models, Models A and B, were found to perform poorly in predicting flow parameters beyond separation. The predictions were markedly improved by the modification of the characteristic length scale used in the turbulence modeling (Model D) for the outer part of the flow. A simplified transport equation for this length scale was proposed. Including turbulence kinetic energy in the turbulence model following the Prandtl-Kolmogorov formulation had little effect on the predictions (Models C and E).

Length scale, rather than turbulence velocity scale, seems to be the parameter which deviates most significantly from equilibrium values in incompressible separating flows, at least as determined by the turbulence models considered in the present study.

3. PREDICTION OF SEPARATED BOUNDARY LAYERS INCLUDING VISCOUS-INVISCID INTERACTION

The presence of flow separation sufficiently alters the inviscid flow over a surface such that neither the viscous nor the inviscid portions of the flow can be computed correctly in an independent manner. Instead, interaction between the viscous and inviscid portions of the flow must be taken into account.

A viscous-inviscid calculation procedure has been developed utilizing the inverse boundary layer finite-difference procedure summarized in the previous section (details are provided in [3]) with a small disturbance Cauchy integral formulation for the inviscid flow. The key features of the inviscid flow calculation and the means of achieving a convergent iterative procedure will be summarized below. More details can be found in [19] and [23].

3.1. Viscous-Inviscid Interaction Analysis

The analysis is applicable for flows containing thin separation bubbles on solid surfaces. It is assumed that the steady boundary layer equations are an adequate mathematical model for the viscous flow and that potential flow theory is adequate for the inviscid flow outside the boundary layer if the displacement effect of the separated region is taken into account. This displacement effect is assumed to be confined to the local neighborhood of the separated flow which will be referred to as the interaction region (see Fig. 2). The concept of a local interaction region has also been used by Jobe [24], Carter and

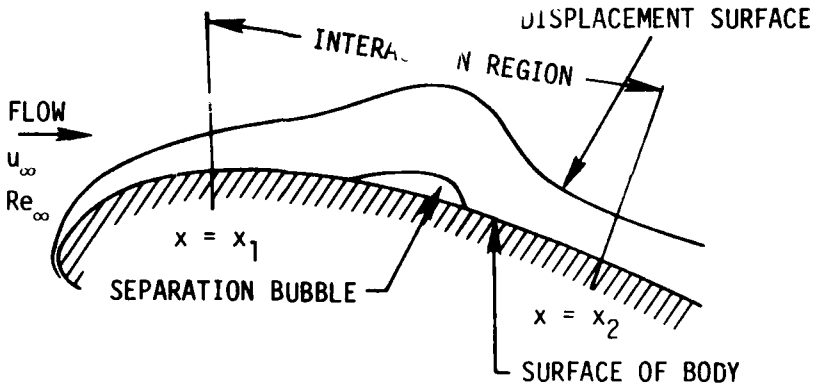

Fig. 2. Schematic diagram of interaction region on a two-dimensional body.

Wornom [4], and others. Within the interaction region the potential flow solution over the displacement surface of the viscous flow significantly differs from the inviscid flow over the solid body alone. Outside the interaction region, conventional boundary layer and potential flow analyses are assumed to be adequate.

The governing equations for the viscous portion of the flow are given by Eqs. (2.1) through (2.6). It is assumed that the inviscid flow is two-dimensional and irrotational, permitting the use of superposition to develop the potential flow solution. Letting $u_{e,o}$ denote the tangential component of velocity of the inviscid flow over the solid body without separation and u_c be the velocity on the displacement surface induced only by the sources and sinks distributed on the surface of the body due to the displacement effect of the viscous flow in the interaction region, the x-component of velocity of a fluid particle on the displacement surface can be written as

$$u_e = u_{e,o} + u_c \tag{3.1}$$

Following Lighthill [25], the intensity of the line source or sink displacing a streamline at the displacement surface of the viscous flow can be evaluated as

$$q = \frac{d(u_e \delta^*)}{dx} \tag{3.2}$$

Using a small disturbance approximation valid for small values of δ^*, $u_c(x)$ can be evaluated as

$$u_c(x) = \frac{1}{\pi} \int_{-\infty}^{\infty} \frac{d(u_e \delta^*)}{dx'} \frac{dx'}{(x - x')} \tag{3.3}$$

More details of this development can be found in [23].

Further details on the calculation of $u_{e,o}$ (the inviscid surface velocity on the body without separation) will not be given here. $u_{e,o}$ can be obtained by conventional methods, for example, by the Hess and Smith [26] procedure or from experimental data. This distribution does not change during the interaction calculation.

The procedure used to match the viscous and inviscid flow solutions in the present study differs somewhat from what is usually considered the "conventional" procedure for flows in which the boundary layer equations cannot be solved by a direct procedure. In the conventional procedure, both the boundary layer and inviscid flows are solved inversely, as in the work reported by Jobe [24] and Carter and Wornom [4]. This conventional method typically requires under-relaxation and a large number of iterations.

In the method developed in the present study, as well as in the method used by Carter in [18], the inviscid solution proceeds in the direct mode utilizing the boundary layer edge velocity and δ^* as an input and providing a new edge velocity as an output. The difference between the edge velocities calculated both ways (from the inviscid and boundary layer procedure) is used as a potential to calculate an improved δ^* distribution. To do this formally, one would seek to determine the way in which a change in edge velocity would influence δ^*. Reasonable success has been achieved by noting that, for low-speed

boundary layer flows, a response to small excursions in local edge velocity tends to preserve the volume flow rate per unit width in the boundary layer, $u_e\delta^* \approx$ constant. This implies that a local decrease in $u_e(x)$ (associated with a more adverse pressure gradient) causes an increase in $\delta^*(x)$, and a local increase in $u_e(x)$ (associated with a more favorable pressure gradient) causes a decrease in $\delta^*(x)$. This trend would appear to agree with experience. The concept is put into practice as follows. Having passed through the boundary layer calculation using $\delta^*_n(x)$ to obtain $u_{e,BL}$ and using $u_{e,BL}$ and δ^*_n in the inviscid calculation to obtain $u_{e,INV}$, the new input to the boundary layer calculation is computed by

$$\delta^*_{n+1} = \delta^*_n\left(\frac{u_{e,BLn}}{u_{e,INVn}}\right) \tag{3.4}$$

It is important to note the Eq. (3.4) only serves as a basis for correcting δ^* between iterative passes, so no formal justification is required as long as the iterative procedure converges. At convergence, $u_{e,BL} = u_{e,INV}$ and Eq. (3.4) represents an identity, thereby having no effect on the nature of the final solution. One of the main advantages of this method is that the need to use "smoothing" or under-relaxation can be avoided; in fact, successive over-relaxation (SOR) can be used. Typically, 1 to 15 iterative passes through the viscous and inviscid procedures where required for convergence of the interaction calculation.

3.2. Turbulence and Transition Modeling

External flows which give rise to thin separation bubbles invariably separate in the laminar state and undergo transition to turbulent flow prior to or coincident with reattachment. Unfortunately there are no known practical procedures for computing the details of laminar-turbulent transition from first principles. An in-depth study of transition has not been included in the present research effort. Instead, the primary objective has been to establish the feasibility of using the present viscous-inviscid interaction approach for transitional bubbles. To do this, the fully turbulent viscosity μ_{ft}, as given by Model D of [3], was multiplied by an empirical intermittency function γ, such that

$$\mu_t = \mu_{ft}\gamma \tag{3.5}$$

Such an approach has proven useful for natural transition on flat surfaces and airfoils [27]. Three schemes for evaluating γ have been applied in the present study.

3.2.1. Transition Model A

The model is described in [19] and is based on existing correlations for natural transition on flat plates and airfoils. Transition was assumed to start when Re_θ equaled or exceeded the value given by Cebeci [27].

$$Re_{\theta,tr} = 1.174 \left[1 + \frac{22400}{Re_x}\right] Re_x^{0.46} \tag{3.6}$$

for

$$0.1 \times 10^6 \leq Re_x \leq 40 \times 10^6$$

For the calculation of the extent of the transition region, the correlation suggested by Chen and Thyson [28] was used:

$$Re_{\Delta x,tr} = A\, Re_{x,tr}^{0.67} \tag{3.7}$$

where A is the function of Mach number expressed by

$$A = 60 + 4.68M_e^{1.92} \tag{3.8}$$

Thus, the extent of the transition region is

$$\Delta x = x_t - x_{tr} = \frac{A\, x_{tr}}{Re_{x,tr}^{0.33}} \tag{3.9}$$

The intermittency function was evaluated using the correlation presented by Dhawan and Narashima [29]. The correlation was obtained based on the source density function of Emmons [30], such as in the streamwise direction

$$\gamma = 1 - \exp(-0.412\, \zeta^2) \tag{3.10}$$

where

$$\zeta = \frac{x - x_{tr}}{\lambda} \tag{3.11}$$

for $x_{tr} \leq x \leq x_t$ and λ is a measure of the extent of the transition region determined in the present study by letting $\gamma = 0.999$, and

$x = x_t$ in Eqs. (3.10) and (3.11). Two potential weaknesses in this model should be pointed out. The transition starting point is computed in a manner which is independent of the location of separation. Poor agreement with measurements might be anticipated if the predicted point for the onset of turbulence does not coincide closely with, and slightly past, the separation point. The second possible problem with this model is the relatively long extent of transition that is predicted. For some bubbles, at least, experimenters report that transition appears to occur nearly instantaneously near the reattachment point.

3.2.2. Transition Model B

The pressure distribution from the separation point to the point where the displacement thickness reaches a maximum is characteristically nearly uniform [31,32]. Transition has frequently been associated with this point of maximum δ^* where the flow "turns down" to reattachment, and experiments tend to confirm that transition is well advanced or completed when reattachment occurs. This point, which marks the end of the constant pressure region in transitional bubbles from several experiments, has been correlated [19] against the Reynolds number at separation. In Transition Model B, transition was assumed to start at the point where constant pressure region ends, which is reasonably well correlated by

$$Re_{x,tr} = 1.0607 Re_{x,s} + 33185 \qquad (3.12)$$

where Re_x is based on the distance from the airfoil stagnation point. Having established the point where transition is initiated by Eq. (3.12), the intermittency function is evaluated by the form suggested by Crimi and Reeves [4]:

$$\gamma = 0, \quad x < x_{tr}$$

$$= 1 - \exp\left[-C_T(x - x_{tr})^2\right], \quad x \geq x_{tr} \tag{3.13}$$

where

$$C_T = 0.025/\delta_s^{*2}$$

3.2.3. Transition Model C

This model assumes that transition occurs instantaneously at the point indicated by Eq. (3.12). Although the model gave surprisingly good results, it was ultimately rejected on physical grounds in that the transition zone was expected to occupy a finite, though possibly very short, region.

3.3. Summary of Results

Table 1 lists the seven separation bubble cases which have been computed to date by the viscous-inviscid interaction method described in this report. Results from the first three cases have been reported elsewhere [19,23]. More recent results will be described in this report.

The study in [19] compared predictions for a laminar test case with the results calculated by Carter and Wornom [4]. The agreement was seen to be quite good. Both Transition Models A and B were used in [19] to predict a midchord transitional separation bubble studied experimentally by Gault [33]. Predictions generally agreed well with the measurements and with the predictions obtained with a different

Table 1. Separation bubble cases computed.

Case	Description	Remarks
1. Carter-Wornom [4] $t = -0.03$	Fully laminar separation bubble on a surface with an indentation, $Re_{\infty,L} = 80{,}000$	Comparisons appear in [19, 23]
2. Gaster [34] Case III, Series II	Transitional separation bubble on a flat surface; pressure gradient generated by airfoil over plate, $Re_s = 3.8 \times 10^5$	Comparisons appear in [23]
3. Gault [33] NACA 66_3-018 airfoil, $\alpha = 0^o$	Transitional midchord separation bubble on an airfoil, $Re_c = 2 \times 10^6$, Tu = 0.15 - 0.2%	Comparisons appear in [19, 23]
4. Gault [33] NACA 66_3-018 airfoil, $\alpha = 2^o$	Transitional midchord separation bubble on an airfoil, $Re_c = 2 \times 10^6$, Tu = 0.15 - 0.2%	Comparisons appear in present report
5. Gault [35] and McCullough and Gault [36] NACA 63-009 airfoil, $\alpha = 4^o$	Transitional leading edge separation bubble on an airfoil, $Re_c = 5.8 \times 10^6$	Comparisons appear in present report
6. Gault [35] and McCullough and Gault [36] NACA 63-009 airfoil, $\alpha = 5^o$	Transitional leading edge separation bubble on an airfoil, $Re_c = 5.8 \times 10^6$	Comparisons appear in present report
7. Gault [35] and McCullough and Gault [36] NACA 63-009 airfoil, $\alpha = 7^o$	Transitional leading edge separation bubble on an airfoil, $Re_c = 5.8 \times 10^6$	Comparisons appear in present report

numerical scheme by Briley and McDonald [17]. There was no clear basis demonstrated in [19] for preferring the predictions of one transition model over the other.

In computing Case 4 of Table 1, a midchord bubble on the NACA 66_3-018 airfoil at a 2^o angle of attack, Transition Model A predicted the onset of transition prior to the experimentally observed separation point and the predicted flow did not separate at all. Transition Model A utilized elements developed for natural transition with very small pressure gradients and was evaluated in order to establish a baseline comparison through which the differences between bubble and natural transition might become evident. Apparently the model predicts an early (compared to experimental results) onset of transition in some cases, which can permit the transitional-turbulent flow to overcome the locally adverse pressure gradient and remain attached, counter to the experimental measurements. Transition Model A was not used further for Cases 4 through 7 in Table 1.

Figures 3, 4, 5, and 6 compare the predicted and measured pressure coefficients for Cases 4-7 in Table 1. The predictions of Crimi and Reeves [15] obtained by an interaction scheme which calculated the viscous flow by an integral method are also shown in Fig. 6. The predicted separation and reattachment points are indicated on the figures. The agreement between the predicted and the measured pressure coefficient appears to be generally good.

Predicted velocity profiles near and in the separated regions are compared with measurements for Cases 4-7 in Figs. 7-10. The agreement

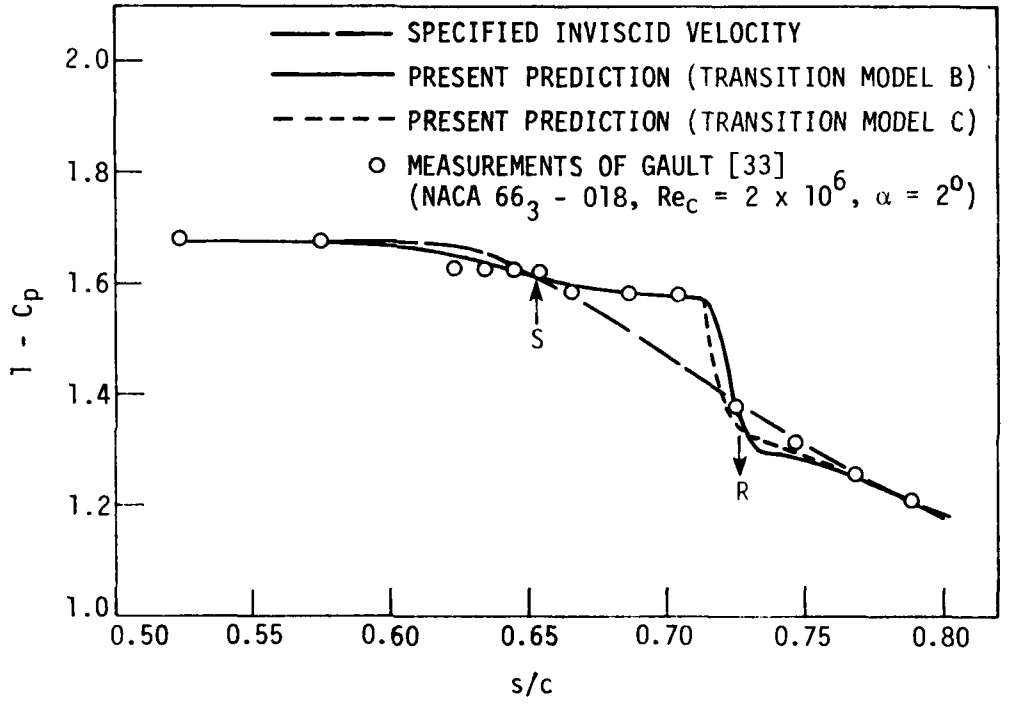

Fig. 3. Comparison of predicted pressure distribution with the experimental data on NACA 66_3-018 airfoil, $\alpha = 2^o$.

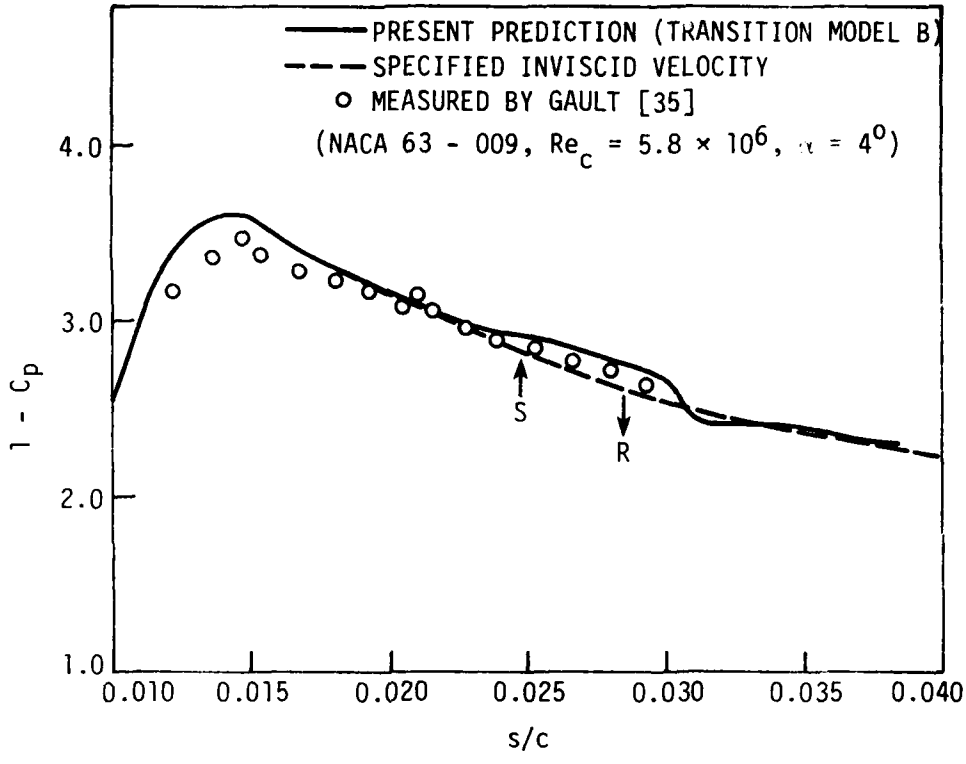

Fig. 4. Comparison of predicted pressure distribution with experimental data on NACA 63-009 airfoil, $\alpha = 4^o$.

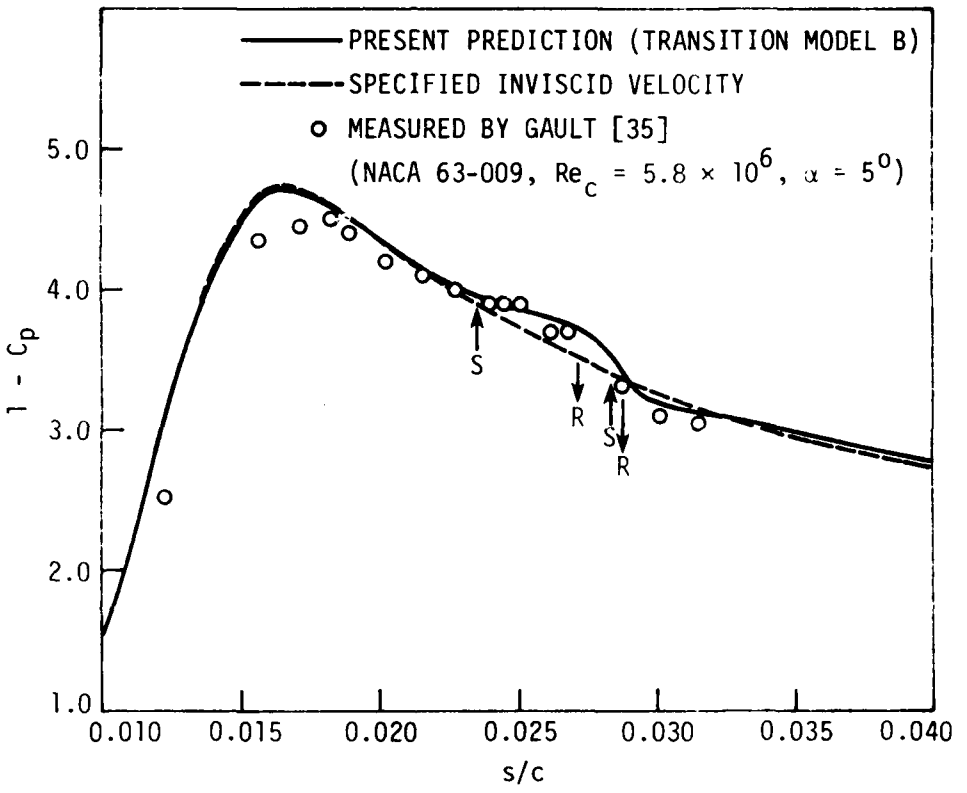

Fig. 5. Comparison of predicted pressure distribution with experimental data on NACA 63 - 009 airfoil, $\alpha = 5^o$.

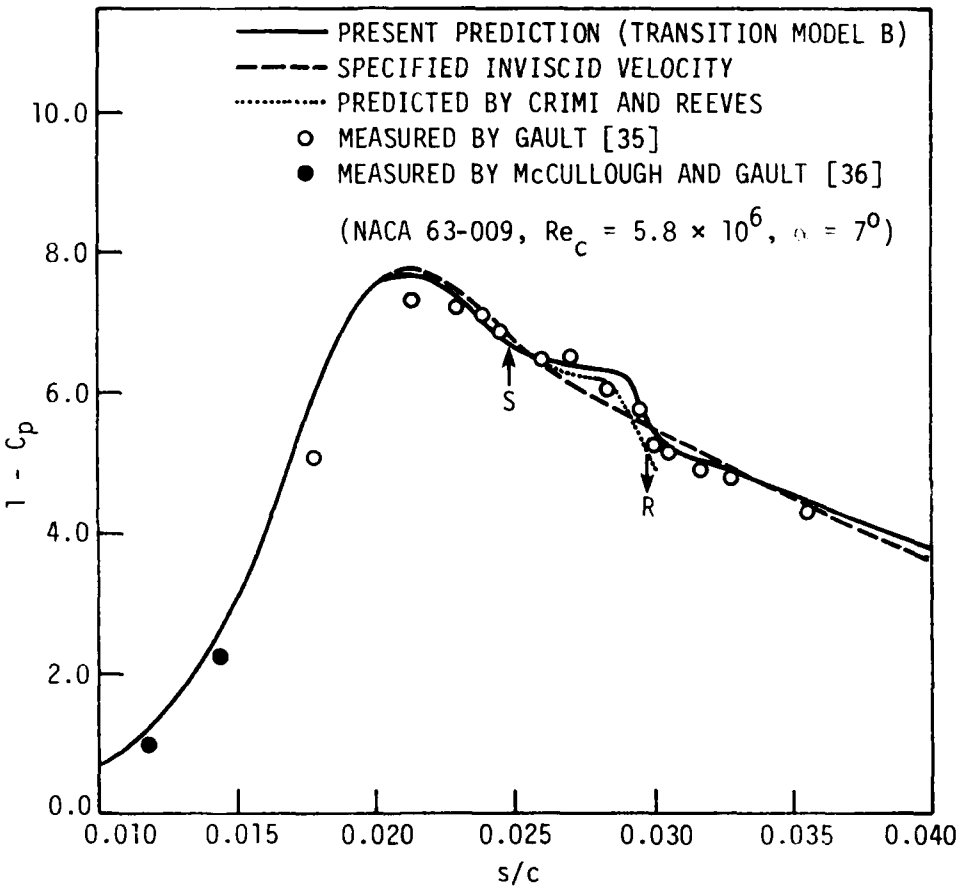

Fig. 6. Comparison of predicted pressure distribution with experimental data on NACA 63-009 airfoil, $\alpha = 7^{o}$.

between predictions and measurements appears reasonable, except, perhaps, for Case 7, the NACA 63-009 airfoil at $\alpha = 7^{o}$. The difficulty of obtaining accurate velocity measurements with conventional pressure probes in and near separated flows is well known [20]. Predicted velocity profiles near reattachment are extremely sensitive to the location of the predicted transition point. For Case 7, especially, the predicted transition occurred slightly downstream of that indicated by the experimental measurements. Here, the steepening of the velocity profiles is taken as evidence of transition from laminar to turbulent flow. Generally, the velocity profiles suggest that the flow separates laminarly and remains essentially laminar until after the local peak in the displacement surface has occurred, indicating that the outer portion of the flow is turning toward the airfoil and that the reversed flow region is shrinking. In one computed case, Case 6, the predicted flow reattached laminarly, separated a second time, underwent transition to turbulent flow, and then reattached a second time. Such behavior is indicated in Fig. 11. Measurements of skin friction are not available for comparison. Despite this unusual predicted flow pattern, the predicted pressure coefficients and velocity profiles are in fairly good agreement with the measurements. It should be remembered that the actual flow near separation and reattachment points is frequently quite complex, with certain portions of the flow fluctuating in time between the separated and attached state [20].

The predictions for Cases 5-7 were for the NACA 63-009 airfoil at increasing angles of attack. The predicted displacement surfaces and

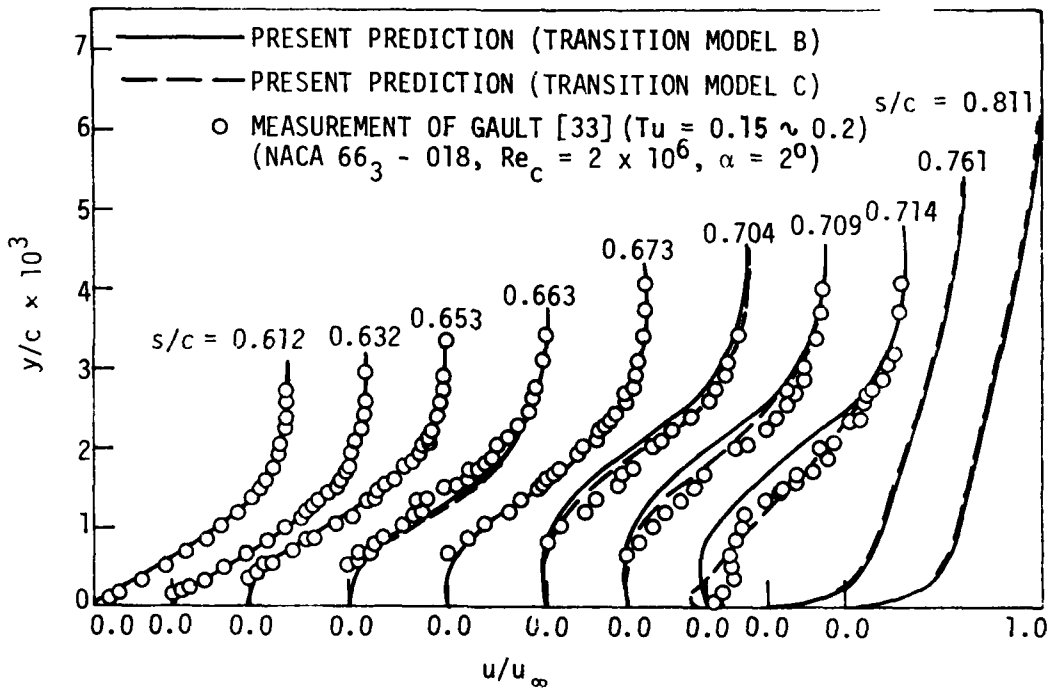

Fig. 7. Comparison of predicted mean velocity profiles with experimental data for NACA 66$_3$ - 018 airfoil, $\alpha = 2^o$.

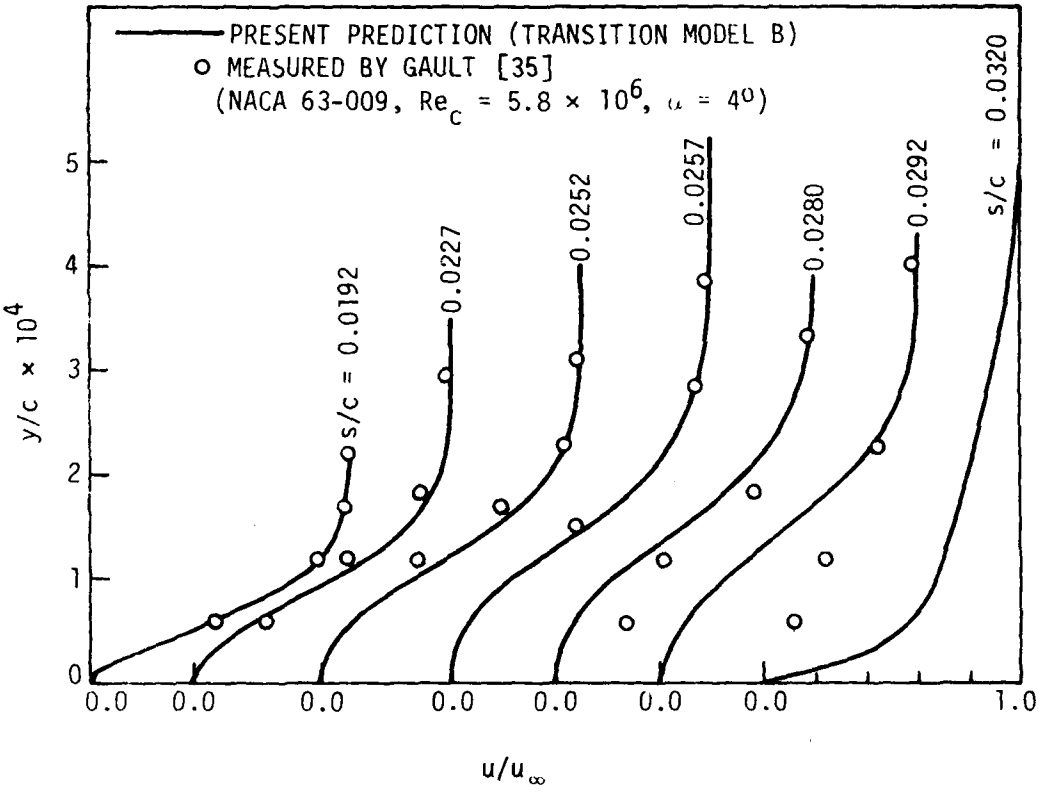

Fig. 8. Comparison of predicted mean velocity profiles with experimental data for NACA 63-009 airfoil, $\alpha = 4^o$.

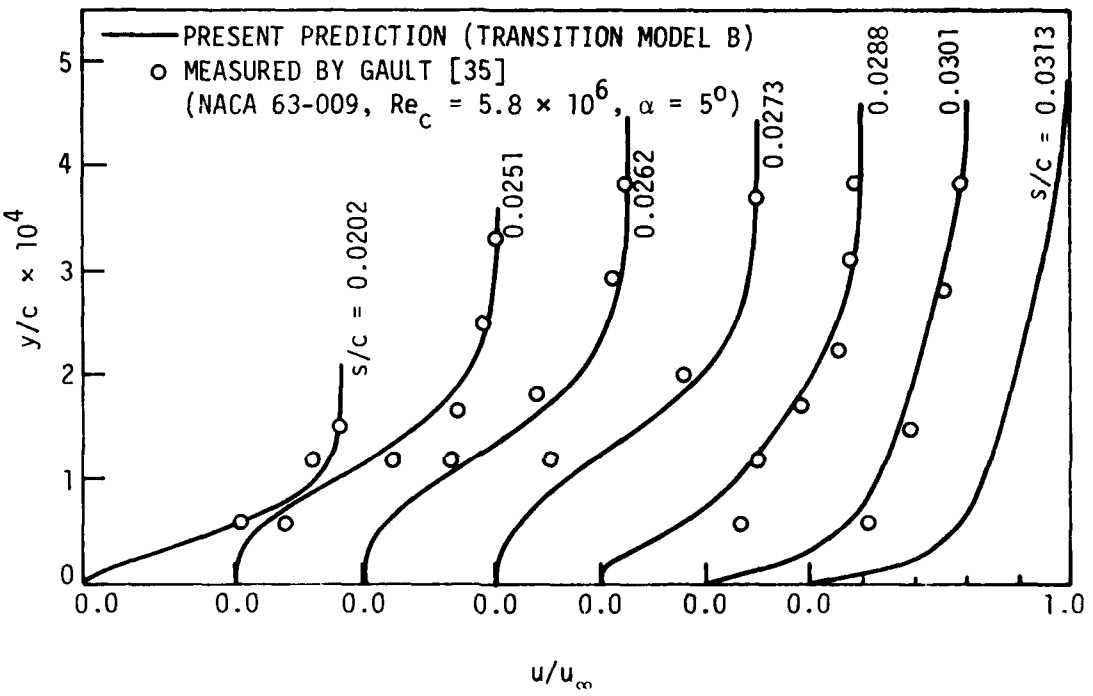

Fig. 9. Comparison of predicted mean velocity profiles with experimental data on NACA 63-009 airfoil, $\alpha = 5^{o}$.

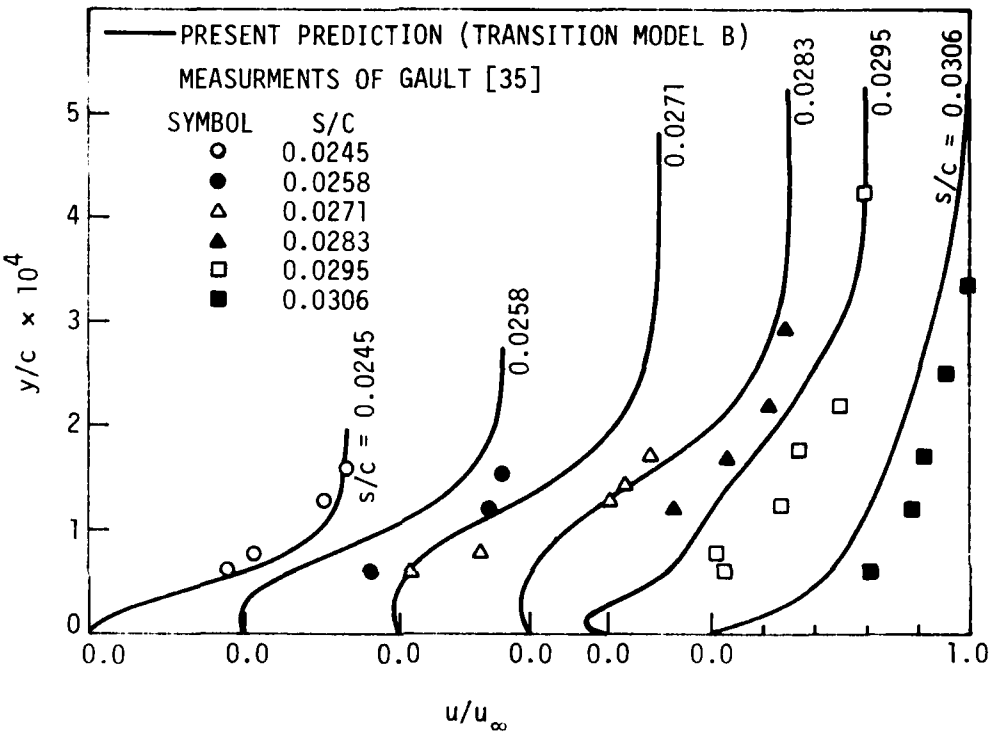

Fig. 10. Comparison of predicted mean velocity profiles with experimental data on NACA 63-009 airfoil, $\alpha = 7^{o}$.

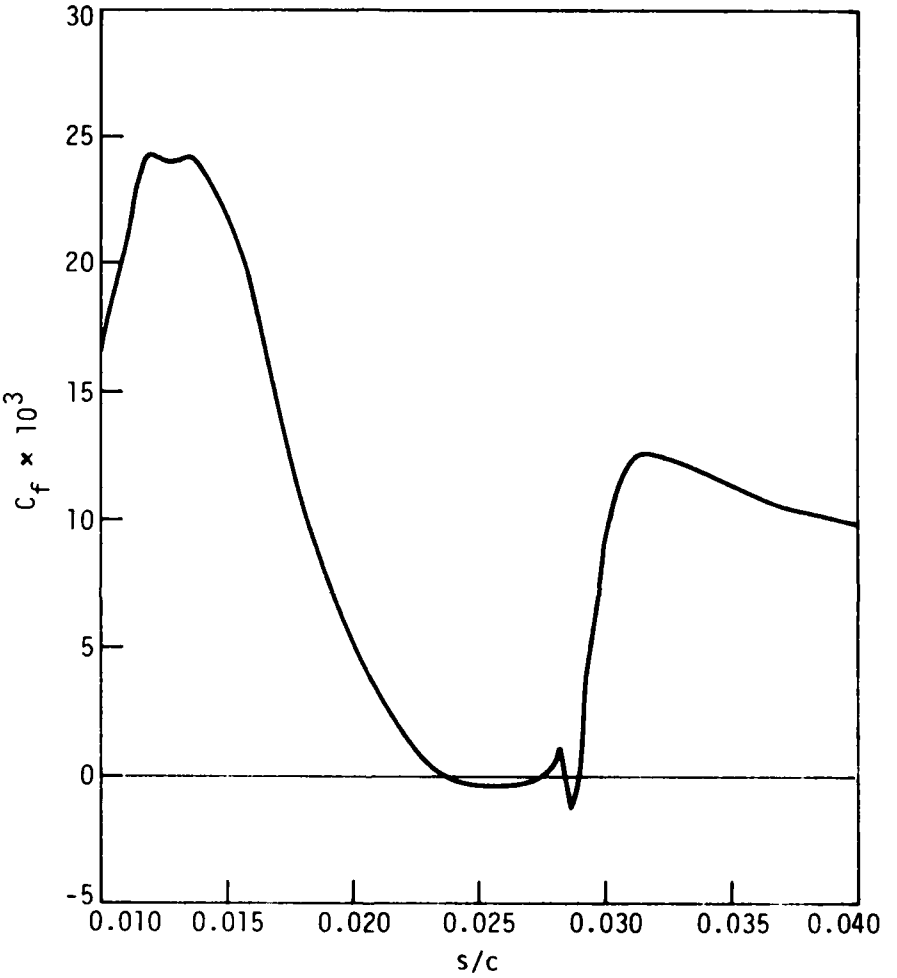

Fig. 11. Distribution of skin friction coefficient on NACA 63-009 airfoil, $Re_c = 5.8 \times 10^6$, $\alpha = 5^o$.

separation and reattachment points for these three cases are shown in Fig. 12. The separation bubble can be seen to move toward the leading edge as the angle of attack increased. This same trend can be observed in the experimental measurements (for example, from the experimental velocity profile of Figs. 4-6), although no displacement thickness was measured to allow a comparison in Fig. 12.

The inviscid velocity distribution for the unseparated flow, needed in the present viscous-inviscid interaction procedure, was obtained by the Hess and Smith [26] procedure for Cases 4-7. From 10 to 15 iterations through the viscous and inviscid calculations were needed for convergence, as determined by the requirement that the maximum change in the inviscid edge velocity be less than 0.6% between two successive iterations. The maximum difference between $u_{e,BL}$ and $u_{e,INV}$ was less than 2%. Computational details for Cases 1-3 can be found in [19] and [23].

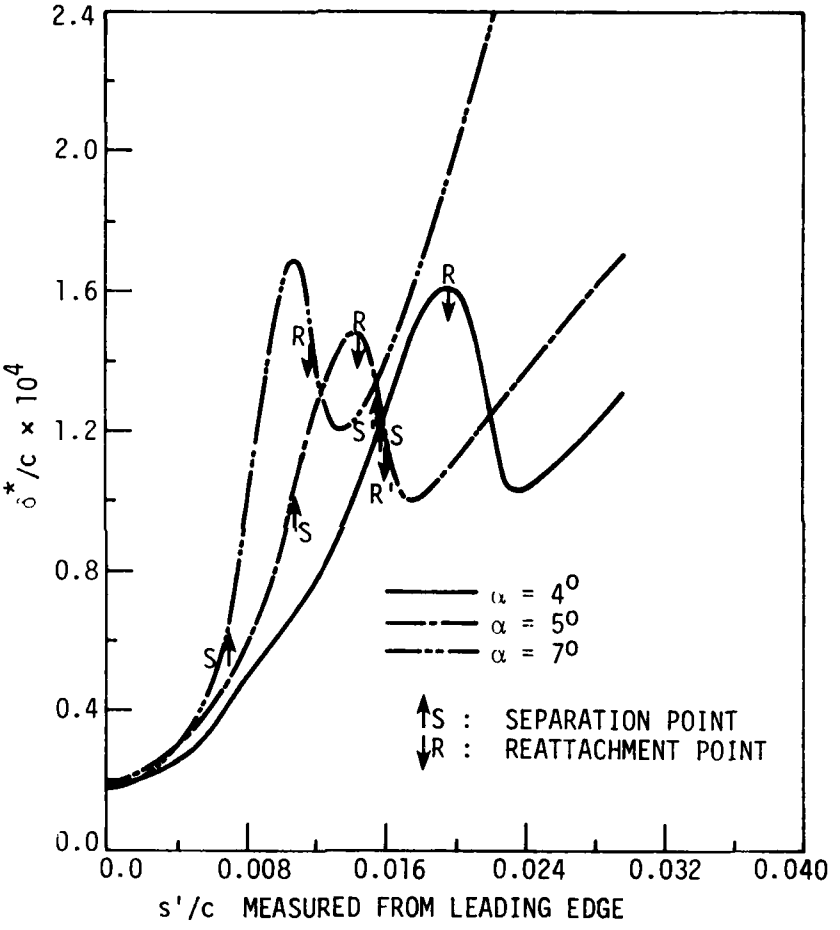

Fig. 12. Variation of displacement distribution with angle of attack on NACA 63-009 airfoil.

4. A SCHEME FOR SOLVING THE PARTIALLY PARABOLIZED NAVIER-STOKES EQUATIONS IN TWO-DIMENSIONAL FLOW

It is desirable in the analysis of any flow problem to determine the simplest mathematical model which will permit a useful prediction. The Navier-Stokes equations stand as the ultimate mathematical model, but the solution of these equations, even by numerical means, is still sufficiently difficult so that interest remains high in identifying simpler mathematical descriptions. Prandtl's boundary layer equations serve as an example of a reduced mathematical model which has proven very useful over the past 75 years. The full range of applicability of the thin shear layer approximation was not evident initially and is even today still being tested. However, there are many common intermediate Reynolds number flows that cannot be adequately represented by Prandtl's boundary layer equations even though they possess a primary flow direction and are without regions of recirculation. The assumptions that upstream influences are negligible and that transverse pressure gradients are small (which are incorporated in the boundary layer equations) tend to mask several important features of these flows.

The boundary layer small-disturbance inviscid interaction calculation method discussed previously appears to be accurate enough for many applications and allows one type of complex flow to be predicted, which could not be treated by conventional boundary layer equations alone. In some applications it is questionable whether the pressure variations in the normal direction through the viscous layer can be ignored. Such flows include separated regions at low Reynolds numbers, flow on highly

curved surfaces and in the neighborhood of abrupt changes in geometry (steps, boat-tails). Higher order calculation schemes that can more accurately account for pressure variations may be needed for accurate prediction of such flows and would enable benchmark comparisons to be made to assess the accuracy of more approximate schemes.

Under motivation as indicated above, work has been initiated to develop a solution procedure for the partially parabolized Navier-Stokes equations. The overall strategy has been to develop a procedure that easily starts with the first pass providing a prediction for zero normal pressure gradients so that for many flows only small changes would be required in successive sweeps. A second requirement has been to use procedures that would readily extend to the full Navier-Stokes equations in those special cases where this would be required.

4.1. Analysis

For a flow predominantly in the x-direction, the partially parabolized equations being solved for a steady, laminar incompressible two-dimensional flow are:

x-momentum

$$u \frac{\partial u}{\partial x} + v \frac{\partial u}{\partial y} = - \frac{1}{\rho} \frac{\partial p}{\partial x} + \nu \frac{\partial^2 u}{\partial y^2} \tag{4.1}$$

y-momentum

$$u \frac{\partial v}{\partial x} + v \frac{\partial v}{\partial y} = - \frac{1}{\rho} \frac{\partial p}{\partial y} + \nu \frac{\partial^2 v}{\partial y^2} \tag{4.2}$$

Continuity

$$\frac{\partial u}{\partial x} + \frac{\partial v}{\partial y} = 0 \tag{4.3}$$

The terms eliminated from the steady Navier-Stokes equations are $(\nu\partial^2 u)/(\partial x^2)$ from Eq. (4.1) and $(\nu\partial^2 v)/(\partial y^2)$ from Eq. (4.2). These terms can be shown (at least formally) to be at least an order of magnitude smaller than those retained for laminar flows in which a predominant flow direction exists. The elimination of these terms removes one source of elliptic behavior from the equations, although the system still is elliptic because of the pressure variation in two directions. In this system, all upstream influences are propagated through the pressure field. To date it has not been possible to make comparisons to determine the computational effort saved by eliminating these two terms from the Navier-Stokes equations. Conceptually, one iteration level has been removed from the system of equations as they have been solved by most schemes. It is probable that the computational effort required is on the order of one-half that required for the full Navier-Stokes equations, perhaps less, and two-dimensional storage is only required for p, rather than for u, v, and p.

The solution procedure will only be outlined briefly here. Further details can be found in [37] and [38]. The procedure utilizes

several concepts from methods already described in the literature, but contains some novel features, especially in the treatment of pressure. The primitive variables of u, v, and p are used with a staggered grid. The only other computational scheme utilizing primitive variables noted to date for solving the partially parabolized system is that of Pratap and Spalding [39].

For a specified pressure field, the system of equations is parabolic, and a solution can be marched in the main flow direction. This solution will not locally satisfy the continuity equation unless the pressure distribution is the "correct" one.

The procedure followed was:

1. An initial guess of $\partial p/\partial y = 0$ was made, and the corresponding $\partial p/\partial x$ was determined for the first computational sweep either to conserve mass on an overall basis (used for the channel calculations in [37]) or according to the boundary layer approximation, $dp/dx = -\rho u_e du_e/dx$ (used for results presented in this report). Starting velocity distributions are specified at the upstream boundary.
2. The u and v components of velocity were calculated at each marching station by a solution of Eq. (4.1) and Eq. (4.2), using the best known values for the pressure.
3. This solution did not, in general, satisfy continuity locally because the pressure field was not the correct one. A corrective flow was found at each marching station by assuming that this corrective flow was irrotational, driven by a velocity

potential as necessary to satisfy the continuity equation [40,41]. The required potential was determined by a single pass of a tridiagonal elimination scheme at each streamwise station. The velocities were then updated by the addition of the corrective flow.

4. In order to move toward the creation of a pressure field that will drive velocities that satisfy continuity locally, a Poisson equation for the pressure was formed from the complete momentum equations using the corrected velocities. The pressure was thereby updated at each streamwise station by relaxing the Poisson equation. It was found useful to store the source term for further global iterations after each streamwise pass.
5. The solution was then advanced to the next streamwise station and Steps 2-4 carried out for each streamwise step in the problem domain. At this point, the entire pressure field has been updated once and the calculation sequence could move to the upstream boundary and a new sweep started, using the improved pressure field. Especially as the solution nears convergence, it has been found helpful to make additional Gauss-Seidel passes through the pressure field (relaxing the Poisson equation) prior to starting the new sweep involving Steps 2-4.

The above procedure differs from the Pracap-Spalding [39] method primarily in the details of Steps 3 and 4 and in the use of iterations

through the pressure field between the computational sweeps to determine velocities.

4.2. Summary of Results

In the comparisons made to date, the solutions to the partially parabolized Navier-Stokes equations have agreed remarkably well with solutions to the full Navier-Stokes equations reported by others. Solutions for developing laminar flow in a channel at low Reynolds numbers are compared with solutions to the full Navier-Stokes equations in [38]. In that study, the predictions from the partially parabolized procedure were observed to be within 5% of the solutions to the full Navier-Stokes equations for Reynolds numbers as low as 10.

More recently, the partially parabolized procedures have been applied to one of the nearly separating external laminar flows studied by Murphy [42] and Briley [43]. The specific case computed can be identified as Run 12 of [42]. This corresponds to Briley Case No. 4 [43], with the distance from the plate to the upper boundary doubled. The flow starts as the classical linearly retarded flow studied by Howarth [44], whereby the outer edge velocity varies according to $u_e = b_0 - b_1 x$, where b_0 and b_1 were taken as 30.48 m/s and 300 s^{-1}, respectively. The kinematic viscosity was $\nu = 1.49 \times 1.0^{-4}$ m^2/s. At $x^* = 0.2$ (with allowance for fairing, as used in [42] and [43]), the outer edge velocity becomes constant at 0.79875 b_0 (see Fig. 13). The outer edge was located at $y = 7.62 \times 10^{-3}$ m (0.025 ft) as in the Murphy Run 12 [42]. The upstream and downstream boundaries were established at $x^* = 0.05$ and $x^* = 0.49$, essentially as in [42] and

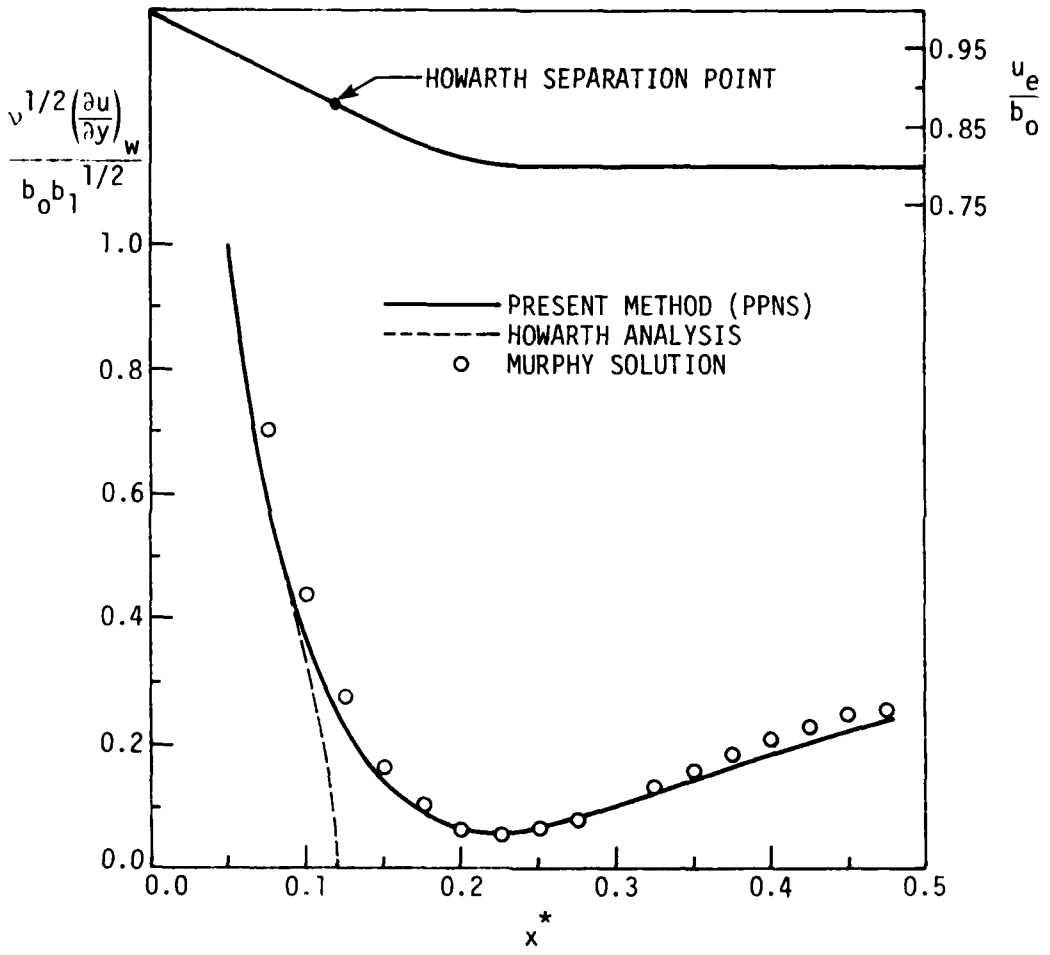

Fig. 13. Comparison of predicted dimensionless skin-friction coefficient, Murphy Run 12 [42].

[43]. The u and v initial ($x^* = 0.05$) velocity distributions were specified to be in agreement with Howarth's boundary layer solutions. Both u_e and v_e were specified at the upper boundary, u_e as indicated above and v_e according to the values obtained by Murphy [45]. No boundary conditions can be imposed at the downstream boundary for the partially parabolized equations.

Murphy [44] utilized a 20 × 18 grid, whereas a 38 × 35 grid was used in the calculations by the present method. The calculations are presently being repeated for a coarser grid to study the effect of mesh size on the solution. Reversed flow was present in the solution during the first few sweeps, but this was readily accommodated in the present marching scheme through the use of the FLARE approximation. Thirty-six streamwise sweeps were required for convergence to the point where the sum of the absolute values of the mass sources in the entire flow field was less than 0.1% of the mass flow rate at the upstream boundary. The calculations required 4.9 minutes on the ITEL AS/6 computer. Additional details on the computational method, which differs considerably from that used by Briley [43] and Murphy [42], can be found in [37] and [38].

The predicted values of skin-friction coefficient are compared with the full Navier-Stokes results obtained by Murphy [45] in Fig. 13. For reference, the skin-friction coefficient from the Howarth [44] solution to the boundary layer equations is also shown in the figure. Conventional boundary layer analysis applied in the direct mode is seen to predict separation at about $x^* = 0.12$. The skin-friction coefficient predicted by the present partially parabolized scheme is

seen to agree fairly well with the Murphy results. The qualitative trends are clearly well predicted by the partially parabolized equations.

Velocity profiles predicted by Murphy and by the present procedure are compared in Fig. 14. The agreement between the two predictions is generally quite good. Both methods predict a slight velocity overshoot near the vicinity of the minimum skin-friction coefficient.

The nondimensional pressure distribution predicted for this flow is shown in Figs. 15 and 16. The reference pressure and velocity in the nondimensional pressure plotted in Fig. 15 correspond to the outer edge values at the downstream boundary where the flow returns to near boundary layer-like conditions. Figure 15 indicates the pressure variation along the flow for four y levels, one very near the surface, one at the outer edge, and two in between. The variation of pressure across the flow is seen to be substantial in the neighborhood of the abrupt change in the outer edge velocity distribution. Pressure profiles across the flow are shown for three x locations in Fig. 16. The results indicate that in the neighborhood of the minimum value of skin friction, the pressure variation across the flow is substantial and not restricted to the outer portion of the flow. Near the downstream boundary, the pressure variation across the viscous portion of the flow is seen to be very small.

The ratio of the transverse to streamwise pressure gradient is plotted across the flow for an x location close to the minimum in skin-friction ($x^* = 0.2253$) in Fig. 17. The normal pressure gradient

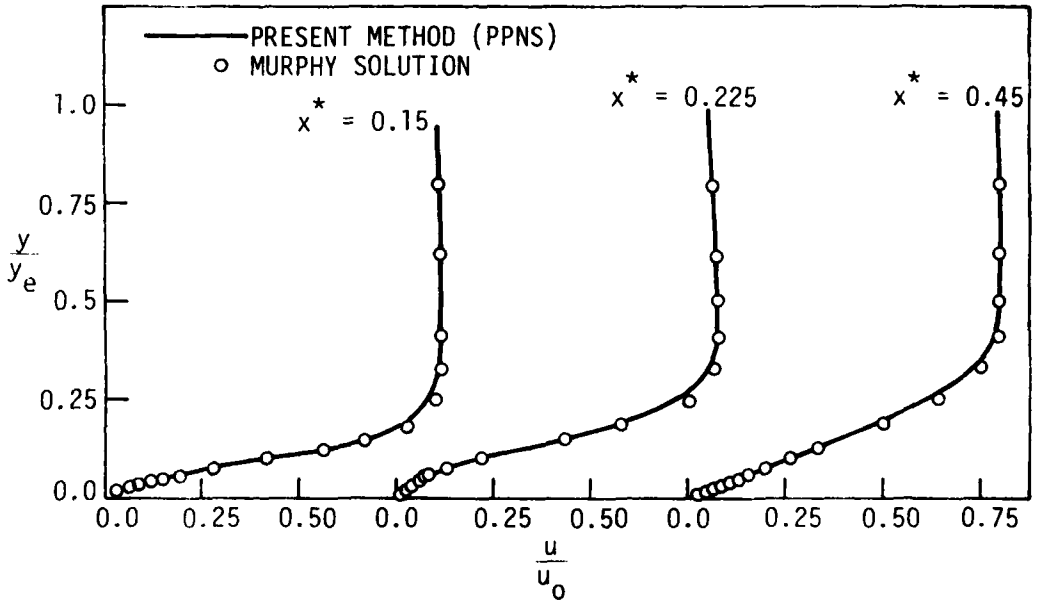

Fig. 14. Comparison of predicted velocity profiles, Murphy Run 12 [42], $u_o = 0.95\ b_o$.

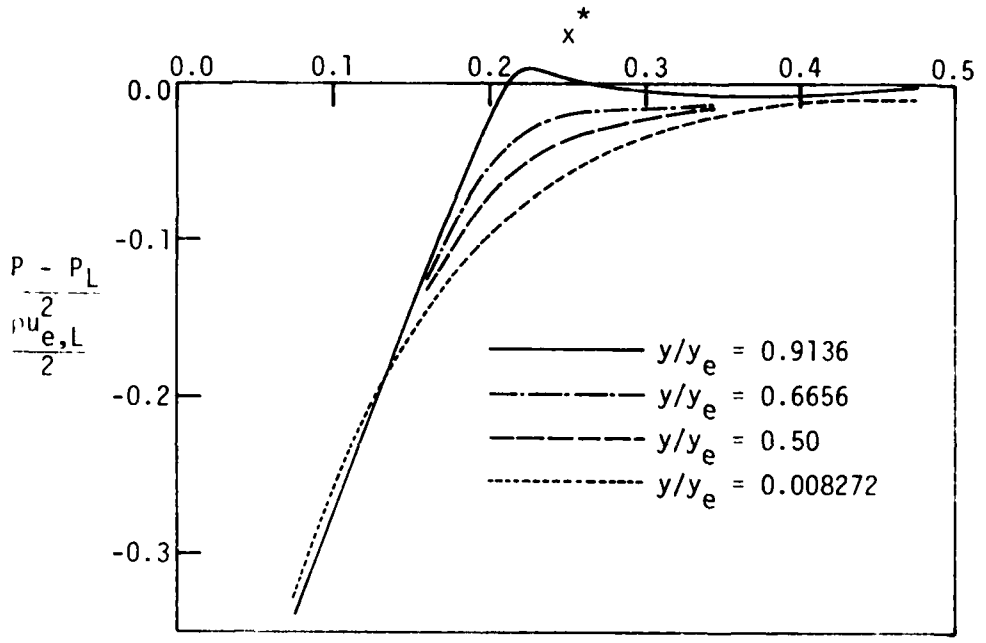

Fig. 15. Predicted nondimensional pressure variation along the flow, Murphy Run 12 [42].

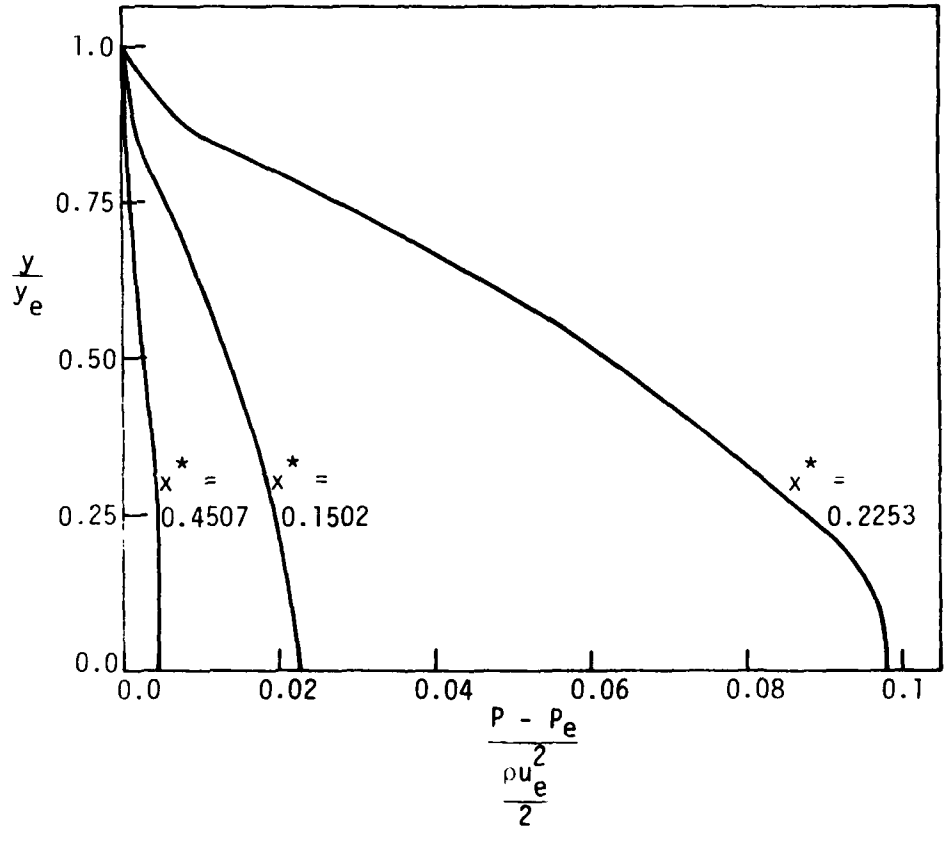

Fig. 16. Predicted nondimensional pressure variation across the flow, Murphy Run 12 [42].

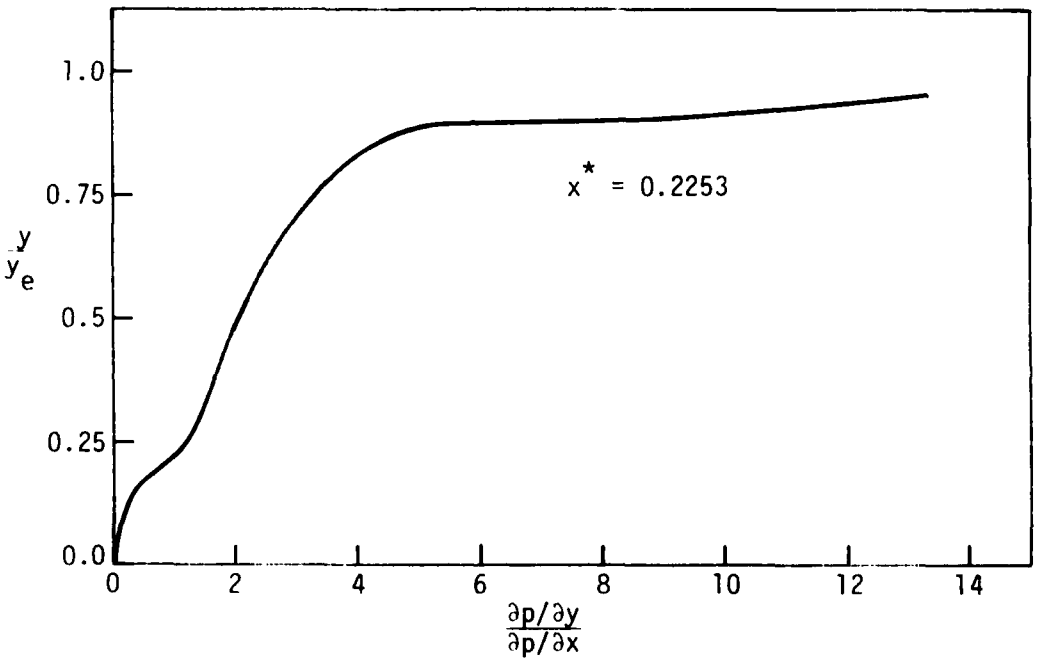

Fig. 17. Predicted ratio of normal to streamwise pressure gradient, $x^* = 0.2253$, Murphy Run 12 [42].

appears to be generally of the same order of magnitude as the streamwise gradient at that location. Although not included in the figure, upstream at $x^* = 0.1502$, the maximum ratio of normal to streamwise pressure gradient was observed to be 0.22, whereas, near the downstream boundary at $x^* = 0.4507$, the maximum ratio was 0.024.

5. CONCLUSIONS

The following are considered the most important conclusions to be drawn from the study which has been summarized in the present report.

1. Quite reasonable predictions of thin separated regions appear possible through an inverse finite-difference boundary layer calculation procedure in which the displacement thickness is specified as a boundary condition rather than the pressure gradient. The solution can be obtained in a once-through computational sweep in the primary flow direction through the use of the FLARE approximation for the streamwise convective derivation.
2. For turbulent flows undergoing separation, standard algebraic turbulence models were found to perform poorly in predicting flow parameters near separation and beyond.
3. Much improved predictions for turbulent separated flow were obtained using a new simplified transport equation for the length scale in the expression for turbulent viscosity in the outer portion of the flow.
4. Including turbulence kinetic energy in the turbulence model for separated flow following the Prandtl-Kolmogorov formulation had little effect on the predictions. Length scale, rather than turbulence velocity scale, seems to be the parameter which deviates most significantly from equilibrium values in incompressible separating flows, at least as determined by the turbulence models considered in the present study.

5. A promising viscous-interaction procedure has been developed for the calculation of external viscous flows containing separation bubbles. The procedure utilizes an inverse finite-difference boundary layer calculation method and a Cauchy integral formulation for the inviscid flow using a small disturbance approximation. This scheme permits computation of the viscous flow in the neighborhood of the separation bubble, starting with the solution for the inviscid flow over the solid body alone as the only input. The new viscous-inviscid matching procedure appears to be well conditioned numerically and overcomes several of the shortcomings associated with earlier matching procedures.
6. Results computed for transitional separation bubbles on airfoils generally agreed well with experimental measurements. The predictions appear quite sensitive to the model used for laminar-turbulent transition. Transition Model B, based on a newly developed correlation for the onset of bubble transition, performed best of the three transition models evaluated.
7. A solution procedure has been developed for the partially parabolized Navier-Stokes equations for incompressible flows which permits the prediction of flows in which transverse pressure gradients may be important, but for which streamwise diffusion of momentum is negligible. The numerical scheme developed appears to work well, convergence always being observed to date for Reynolds numbers ranging from 0.5 to

10,000. The rapid convergence is thought to be due to the formulation used for the pressure, especially the use of a Poisson equation which accounts for all terms in the momentum equations.

8. Solutions to the partially parabolized equations for developing flow in a channel at Reynolds numbers as low as 10 and for a nearly separating laminar external flow over a plate at $Re_L \simeq 10{,}000$ were seen to agree remarkably well with solutions to the full Navier-Stokes equations. From this it can be concluded that streamwise diffusion of momentum is often a negligible process even at low Reynolds numbers and that most of the discrepancy between the boundary layer and Navier-Stokes solutions can be eliminated by accounting for nonzero transverse pressure gradients.

9. In the nearly separating laminar external flow case, the numerical solutions to the partially parabolized Navier-Stokes equations indicate a substantial pressure variation in the normal direction near the location of the minimum in skin friction. The variation was not confined to the outer portions of the flow. It is not known whether this variation is highly dependent on the Reynolds number and outer boundary conditions of the flow or whether it is a generally occurring phenomena for flows approaching separation. It would be interesting to test the boundary layer small-disturbance inviscid interaction flow model for a flow such as this, in which the solution to

the more complete flow model indicated such a large variation in pressure in the normal direction.

6. ACKNOWLEDGMENTS

This research was supported by the Engineering Research Institute of Iowa State University through funds provided by the U.S. Army Research Office under Grant DAAG-29-76-G-0155. The authors are grateful for the able assistance provided by Mr. Nateri K. Madavan during the final stages of the work.

7. REFERENCES

1. Goldstein, S., "On Laminar Boundary Layer Flow Near a Position of Separation," Q. J. Mech. Appl. Math., 1:43-69 (1948).

2. Pletcher, R. H. and Dancy, C. L., "A Direct Method of Calculating Through Separated Regions in Boundary Layer Flow," Trans. ASME, J. Fluids Eng., 98:568-572 (1976).

3. Pletcher, R. H., "Prediction of Incompressible Turbulent Separating Flow," Trans. ASME, J. Fluids Eng., 100:427-433 (1978).

4. Carter, J. E. and Wornom, S. F., "Solutions for Incompressible Separated Boundary Layers Including Viscous-Inviscid Interaction," NASA SP347, Aerodynamic Analyses Requiring Advanced Computers, Part I, 125-150 (1975).

5. Cebeci, T., "Separated Flows and Their Representation by Boundary Layer Equations," Report ONR-CR215-234-2, Office of Naval Research, Arlington, Va. (1976).

6. Ghose, S. and Kline, S. J., "Prediction of Transitory Stall in Two-Dimensional Diffusers," Report MD-36, Dept. of Mech. Engr., Stanford University (1976).

7. Moses, H. L., Jones, R. R. III and O'Brien, W. F. Jr., "Simultaneous Solution of the Boundary Layer and Freestream with Separated Flow," AIAA J., 16(3):61-66 (1978).

8. Reyhner, T. A. and Flügge-Lotz, I., "The Interaction of a Shock Wave with a Laminar Boundary Layer," Int. J. Non-Linear Mech., 3(2):173-199 (1968).

9. Klineberg, J. M. and Steger, J. L., "On Laminar Boundary Layer Separation," AIAA Paper No. 74-94 (1974).

10. Carter, J. E., "Solutions for Laminar Boundary Layers with Separation and Reattachment," AIAA Paper No. 74-583 (1974).

11. Arieli, R. and Murphy, J. D., "Pseudo-Direct Solutions to the Boundary-Layer Equations for Separated Flow," AIAA Paper No. 79-0139 (1979).

12. Cebeci, T., Keller, H. B. and Williams, P. G., "Separating Boundary-Layer Flow Calculations," J. Comput. Phys., 31:363-378 (1979).

13. Wooley, R. L. and Kline, S. J., "A Procedure for Computation of Fully Stalled Flows in Two-Dimensional Passages," Trans. ASME, J. Fluids Eng., 100:180-186 (1978).

14. Kim, J., Kline, S. J. and Johnston, J. P., "Investigation of Separation and Reattachment of a Turbulent Shear Layer: Flow Over a Backward Facing Step," Report MD-37, Dept. of Mech. Engr., Stanford University (1978).

15. Crimi, P. and Reeves, B. L., "Analysis of Leading-Edge Separation Bubbles on Airfoils," AIAA J., 14(11):1548-1555 (1976).

16. Gerhart, P. M. and Chima, R. V., "Development of a Method for Predicting Subsonic Turbulent Separating Boundary Layers," Final Report, Dept. of Mech. Engr., University of Akron, Akron, Ohio (1978).

17. Briley, W. R. and McDonald, H., "Numerical Prediction of Incompressible Separation Bubbles," J. Fluid Mech., 69(4):631-656 (1975).

18. Carter, J. E., "A New Boundary-Layer Interaction Technique for Separated Flows," NASA Tech. Mem. 78690 (1978).

19. Kwon, O. K. and Pletcher, R. H., "Prediction of Incompressible Separated Boundary Layers Including Viscous-Inviscid Interaction," Trans. ASME, J. Fluids Eng., 101:466-472 (1979).

20. Simpson, R. L., Strickland, J. H. and Barr, P. W., "Laser and Hot Film Anemometer Measurements in a Separating Turbulent Boundary Layer," Technical Report WT-3, Southern Methodist University, Thermal and Fluid Sciences Center (1974).

21. Chu, J. and Young, A. D., "Measurements in Separating Two-Dimensional Turbulent Boundary Layers," AGARD Conference Proceedings No. 168, Flow Separation, 13-1 to 13-12 (1975).

22. Pletcher, R. H., "Prediction of Turbulent Boundary Layers at Low Reynolds Numbers," AIAA J., 14(5):696-698 (1976).

23. Kwon, O. K. "Prediction of Incompressible Boundary Layers Including Viscous-Inviscid Interaction," MS Thesis, Iowa State University, Ames (1978).

24. Jobe, C. E., "The Numerical Solution of the Asymptotic Equations of Trailing Edge Flow," Tech. Report AFFDL-TR-74-46, Air Force Flight Dynamics Laboratory (1974).

25. Lighthill, M. J., "On Displacement Thickness," J. Fluid Mech., 4:383-392 (1958).

26. Hess, J. L. and Smith, A. M. O., "Calculation of Potential Flow About Arbitrary Bodies," Progress in Aeronautical Sciences, 8:1-138 (1967).

27. Cebeci, T., Mosinskis, G. J. and Smith, A. M. O., "Calculation of Viscous Drag and Turbulent Boundary-Layer Separation on Two-Dimensional and Axisymmetric Bodies in Incompressible Flows," Report No. MDC J0973-01, Douglas Aircraft Co., Long Beach, California (1970).

28. Chen, K. K. and Thyson, N. A., "Extension of Emmons' Spot Theory to Flows on Blunt Bodies," AIAA J., 9(5):821-825 (1971).

29. Dhawan, S. and Narashima, R., "Some Properties of Boundary Layer Flows during the Transition from Laminar to Turbulent Motion," J. Fluid Mech., 3(4):418-436 (1958).

30. Emmons, H. W., "The Laminar-Turbulent Transition in a Boundary Layer-Part I," J. Aerosp. Sci., 18(7):235-246 (1951).

31. Ward, J. W., "The Behavior and Effects of Laminar Separation Bubbles on Aerofoils in Incompressible Flow," J. R. Aeronaut. Soc., 67:783-790 (December 1963).

32. Horton, H. P., "A Semi-Empirical Theory for the Growth and Bursting of Laminar Separation Bubbles," United Kingdom Aeronautical Research Council, Current Paper No. 1073 (1969).

33. Gault, D. E., "An Experimental Investigation of Regions of Separated Laminar Flow," NACA TN-3505 (1955).

34. Gaster, M., "The Structure and Behavior of Laminar Separation Bubbles," AGARD Conference Proceedings No. 4, Separated Flows, Part 2, Technical Editing and Reproduction Ltd., London, 813-854 (1966).

35. Gault, D. E., "Boundary Layer and Stalling Characteristics of the NACA 63-009 Airfoil Section," NACA TN 1894 (1949).

36. McCullough, G. B. and Gault, D. E., "Examples of Three Representative Types of Airfoil Section Stall at Low Speed," NACA TN 2502 (1951).

37. Chilukuri, R., "A Calculation Procedure for the Partially Parabolized Navier-Stokes Equations in Primitive Variables for Steady Two-Dimensional Flow," MS Thesis, Iowa State University, Ames (1979).

38. Chilukuri, R. and Pletcher, R. H., "Numerical Solutions to the Partially Parabolized Navier-Stokes Equations for Developing Flow in a Channel," paper submitted for publication to Numerical Heat Transfer (1979).

39. Pratap, V. S. and Spalding, D. B., "Fluid Flow and Heat Transfer in Three-Dimensional Duct Flows," Int. J. Heat Mass Transfer, 19:1183-1188 (1976).

40. Briley, W. R., "Numerical Method for Predicting Three-Dimensional Flows in Ducts," J. Comput. Phys., 14:8-28 (1974).

41. Ghia, V., Ghia, K. N. and Struderuss, C. J., "Three-Dimensional Laminar Incompressible Flow in Straight Polar Ducts," Comput. Fluids, 5:205-218 (1977).

42. Murphy, J. D., "An Efficient Solution Procedure for the Incompressible Navier-Stokes Equations," AIAA J., 15(9):1307-1314 (1977).

43. Briley, W. R., "A Numerical Study of Laminar Separation Bubbles Using the Navier-Stokes Equations," J. Fluid Mech., 47:713-736 (1971).

44. Howarth, L., "On the Solution of the Laminar Boundary Layer Equations," Proc. R. Soc., 64:547-579 (1938).

45. Murphy, J. D., Personal Communication (1978).

APPENDIX A. LIST OF SCIENTIFIC PERSONNEL

R. H. Pletcher, Principal Investigator, Professor of Mechanical Engineering

M. R. Malik, Research Assistant, 1976

S. S. Hwang, Research Assistant, 1976

O. K. Kwon, Research Assistant 1977-1979, MS Degree awarded in May 1978

R. Chilukuri, Research Assistant 1977-1979, MS Degree awarded in May 1979

N. K. Madavan, Research Assistant, 1979

APPENDIX B. LIST OF PUBLICATIONS RESULTING FROM GRANT RESEARCH

In addition to the present report, the following journal articles and technical paper presentations were based on research supported through Grant DAAG29-76-G-0155 from the Army Research Office.

1. Pletcher, R. H., "Prediction of Incompressible Turbulent Separating Flow," ASME Paper No. 78-WA/FE-4, presented at the ASME Winter Annual Meeting, San Francisco, California, December 1978.

2. Pletcher, R. H., "Prediction of Incompressible Turbulent Separating Flow," Trans. ASME, Journal of Fluids Engineering, 100, pp. 427-433, 1978.

3. Kwon, O. K. and Pletcher, R. H., "Prediction of Incompressible Separated Boundary Layer Including Viscous-Inviscid Interaction," paper presented at the Symposium on Turbulent Boundary Layers at the Joint ASME-CSME Applied Mechanics, Fluids Engineering and Bioengineering Conference, Niagara Falls, New York, June 1979 (published in the symposium proceedings).

4. Kwon, O. K. and Pletcher, R. H., "Prediction of Incompressible Separated Boundary Layers Including Viscous-Inviscid Interaction," Trans. ASME, Journal of Fluids Engineering, 101, pp. 466-472, 1979.

5. Chilukuri, R. and Pletcher, R. H., "Numerical Solutions to the Partially Parabolized Navier-Stokes Equations for Developing Flow in a Channel," paper submitted for publication to Numerical Heat Transfer, 1979.